Title	Differential interactions between transforming growth factor-β3/TβR1, TAB1, and CD2AP disrupt blood-testis barrier and sertoli-germ cell adhesion
Author(s)	Xia, W; Mruk, DD; Lee, WM; Cheng, CY
Citation	Journal Of Biological Chemistry, 2006, v. 281 n. 24, p. 16799-16813
Issued Date	2006
URL	http://hdl.handle.net/10722/48684
Rights	Journal of Biological Chemistry. Copyright © American Society for Biochemistry and Molecular Biology, Inc.

THE JOURNAL OF BIOLOGICAL CHEMISTRY VOL. 281, NO. ??, pp. 1–xxx, ???? ??, 2006

Differential Interactions between Transforming Growth Factor-β3/TβR1, TAB1, and CD2AP Selectively Disrupt Blood-Testis Barrier and Sertoli Germ Cell Adhesion*

Received for publication, February 21, 2006, and in revised form, April 13, 2006 Published, JBC Papers in Press, April 13, 2006, DOI 10.1074/jbc.M601618200

Weiliang Xia[‡], Dolores D. Mruk[‡], Will M. Lee[§], and C. Yan Cheng[‡1]

From the [‡]Population Council, Center for Biomedical Research, New York, New York 10021 and [§]Department of Zoology, University of Hong Kong, Hong Kong, China

The biochemical basis that regulates the timely and selective opening of the blood-testis barrier (BTB) to migrating preleptotene/leptotene spermatocytes at stage VIII of the epithelial cycle in adult rat testes is virtually unknown. Recent studies have shown that cytokines (*e.g.* transforming growth factor (TGF)-β3) may play a crucial role in this event. However, much of this information relies on the use of toxicants (*e.g.* $CdCl_2$), making it difficult to relay these findings to normal testicular physiology. Here we report that overexpression of TGF-β3 in primary Sertoli cells cultured *in vitro* indeed perturbed the tight junction (TJ) barrier with a concomitant decline in the production of BTB constituent proteins as follows: occludin, N-cadherin, and ZO-1. Additionally, local administration of TGF-β3 to testes *in vivo* was shown to reversibly perturb the BTB integrity and Sertoli germ cell adhesion via the p38 MAPK and ERK signaling pathways. Most importantly, the simultaneous activation of p38 and ERK signaling pathways is dependent on the association of the TGF-β3-TβR1 complex with adaptors TAB1 and CD2AP because if TβR1 was associated preferentially with CD2AP, *only* Sertoli germ cell adhesion was perturbed without compromising the BTB. Collectively, these data illustrate that local production of TGF-β3, and perhaps other TGF-βs and cytokines, by Sertoli and germ cells into the microenvironment at the BTB during spermatogenesis transiently perturbs the BTB and Sertoli germ cell adhesion to facilitate germ cell migration when the activated TβRI interacts with adaptors TAB1 and CD2AP. However, TGF-β3 selectively disrupts Sertoli germ cell adhesion in the seminiferous epithelium to facilitate germ cell migration without compromising BTB when TβRI interacts only with adaptor CD2AP.

In adult mammalian testes, such as rats, the blood-testis barrier (BTB)[2] is one of the "tightest" barriers in the mammalian body, comparable with the blood-brain barrier (1–3). Yet the BTB must "open" (or restructure/disassemble) at stages VII–VIII of the epithelial cycle to accommodate the migration of preleptotene and leptotene spermatocytes across the barrier but remain "closed" at other stages throughout spermatogenesis (4). Although detailed morphological studies of the BTB were unraveled in the 1960s (5, 6), it remains a biological mystery regarding how germ cells can traverse the BTB while the barrier function is maintained during spermatogenesis. This is largely because of the lack of a suitable *in vivo* model in the field to study BTB dynamics. Recent studies have illustrated that the Sertoli cell tight junction (TJ) permeability barrier is regulated, at least in part, by testosterone (7, 8), possibly via its effects on the steady-state levels of occludin and ZO-1 (7) at the BTB. Furthermore, the BTB is utilizing a unique "engagement" and "disengagement" mechanism between adherens junction (AJ) and TJ to facilitate germ cell movement in which AJs (*e.g.* basal ectoplasmic specialization (ES), a testis-specific cell-cell actin-based AJ type) can be transiently disrupted without compromising the TJ barrier (9, 10). Yet the biochemical mechanism that induces transient TJ "opening" to facilitate germ cell migration is not known. Recent studies have shown that TGF-β3 administered to Sertoli cells cultured *in vitro* could perturb the TJ barrier by reducing the protein levels of occludin and ZO-1 (11). Interestingly, the cadmium-induced BTB restructuring *in vivo* was also associated with an induction of TGF-β3 and an activation of the p38 MAPK concomitant with a reduction in the protein levels of occludin/ZO-1 and N-cadherin/β-catenin at the BTB (12). Although results of these *in vivo* studies were obtained by using animal models involving toxicants, such as $CdCl_2$, they have implicated the crucial role of TGF-β3 in BTB regulation. Because Sertoli and germ cells are both known to produce TGF-β3 (13, 14), we hypothesize that this cytokine released locally to the microenvironment at the BTB may indeed be used to regulate the opening of TJ at stage VIII of the epithelial cycle via the p38 MAPK pathway. Furthermore, a recent study has illustrated that TGF-β3 limits its action at the AJ (*e.g.* apical ES) without perturbing the BTB integrity when only the ERK signaling pathway is activated (15). We speculate that a unique mechanism is in place involving adaptors, such as CD2AP (CD2-associated protein) and TAB1 (TAK1-binding protein) (14), which selects the downstream signaling events of TGF-β3 so that it either induces restructuring at the BTB and Sertoli germ cell adhesion or limits its effects on cell adhesion without perturbing the BTB integrity. We thus sought to delineate the intriguing interactions between the TGF-β3-TβRI protein complex and the two adaptors, CD2AP and TAB1, in the testis, and how these interactions selectively activated the downstream signal transducers of TGF-β3, which, in turn, led to restructuring at the BTB and/or Sertoli germ cell interface. The testis apparently is using such a novel mechanism to regulate restructuring at the Sertoli germ cell interface to facilitate germ cell movement across the epithelium during spermatogenesis while maintaining the BTB integrity. In the course of this investigation, we have also unraveled a potentially useful *in vivo* model to study BTB dynamics.

* This work was supported in part by NICHD Grants U01 HD045908 and U54 HD029990, Project 3 (to C. Y. C.), from the National Institutes of Health and CONRAD Program Grant CICCR, C1G 01-72. The costs of publication of this article were defrayed in part by the payment of page charges. This article must therefore be hereby marked "*advertisement*" in accordance with 18 U.S.C. Section 1734 solely to indicate this fact.

[1] To whom correspondence should be addressed: Population Council, 1230 York Ave., New York, NY 10021. Fax: 212-327-8733; E-mail: Y-Cheng@popcbr.rockefeller.edu.

[2] The abbreviations used are: BTB, blood-testis barrier; JNK, c-Jun NH_2-terminal kinase; Co-IP, co-immunoprecipitation; RT, reverse transcription; TGF, transforming growth factor; MAP, mitogen-activated protein; MAPK, MAP kinase; ERK, extracellular signal-regulated kinase; TJ, tight junction; AJ, adherens junction; ES, ectoplasmic specialization; ANOVA, analysis of variance; ER, endoplasmic reticulum; TER, transepithelial electrical resistance; SC, Sertoli cell.

TABLE 1

A summary of experiments conducted in this laboratory for the past 2 years illustrating the transfection efficiency in overexpressing TGF-β3 with different vectors in primary cultures of Sertoli cells

Vector[a]	Transfection method tested (no. of experiments conducted excluding preliminary experiments)	Transfection efficiency	Refs.
		%	
pGL3-Control and pRL-TK	Calcium phosphate co-precipitation ($n = 2$)	ND	50–52
pCIneo/TGF-β3	Calcium phosphate co-precipitation ($n = 4$)	14.9 ± 1.6	
pTracer-CMV2/TGF-β3	Calcium phosphate co-precipitation ($n = 3$)	12.4 ± 3.1	
pGL3-Control and pRL-TK	Effectene ($n = 2$)	ND	53
pCIneo/TGF-β3	Effectene ($n = 6$)	15.5 ± 2.8	

[a] All vectors were purchased from Promega except pTracer-CMV2, which was obtained from Invitrogen. ND indicates not determined.

EXPERIMENTAL PROCEDURES

Animals—Sprague-Dawley rats were purchased from Charles River Breeding Laboratories (Kingston, NY) and were housed at the Rockefeller University Laboratory Animal Research Center with a 12:12-h light/dark cycle with free access to water and standard chow. The use of Sprague-Dawley rats for the studies described here was approved by the Rockefeller University Animal Care and Use Committee with Protocol Numbers 03017, 03040, and 06018.

Transient Transfection of Primary Sertoli Cell Cultures with Plasmid Containing TGFβ3 cDNA and the Effects on Sertoli Cell TJ Permeability Barrier—pCI-neo mammalian expression vector (Promega) containing the full-length sequence encoding rat TGF-β3 was prepared using the following specific primers (GenBank™ accession number NM_013174): 5′-CTGGCCTCGTTCCTG**AA**TTCACACATGAAGATG-3′ (sense, 375–407); 5′-TTCGCCTCCTCTGTT**CT**AGACTGGCCTCAGCT-3′ (antisense, 1663–1632). Two bases (boldface) were mutated to create the corresponding EcoRI and XbaI cloning sites (underlined). The authenticity of this full-length clone was confirmed by direct nucleotide sequencing prior to its use for subsequent experiments. For transient transfection, Sertoli cells were isolated from 20-day-old rat testes to a purity of greater than 95% as described previously (11, 16). Sertoli cells were seeded on Matrigel-coated (diluted 1:5 with F-12/Dulbecco's modified Eagle's medium; BD Biosciences) bicameral units (Millicell HA filters, Millipore Corp.), 12-well plates, or cover glass at a density of $1.2 \times 10^6/cm^2$, $0.5 \times 10^6/cm^2$, or $0.15 \times 10^6/cm^2$, respectively, and cultured in F-12/Dulbecco's modified Eagle's medium at 35 °C in a humidified atmosphere of 95% air, 5% CO_2. Transfection was carried out 2 days after isolation, using Effectene Transfection Reagent (Qiagen) with ~0.3 μg of plasmid DNA/6×10^5 Sertoli cells (plasmid/enhancer (μg/μl) and plasmid/Effectene Reagent (μg/μl) were 1:8 and 1:15, respectively) following the protocols provided by Qiagen with a transfection efficiency of ~15% (see Table 1). Cells were incubated for an additional 24 h in the transfecting mixture, and fresh F-12/Dulbecco's modified Eagle's medium was replaced. In preliminary experiments to optimize transfection efficiency using either calcium phosphate co-precipitation or Effectene reagent (Qiagen) (see Table 1), luciferase reporter plasmid (pGL3-Control and pRL-TK; Promega) was co-transfected into Sertoli cells with various combinations on the amounts of plasmid DNA (~0.1–3 μg), different cell densities ($0.1–1.2 \times 10^6$ cells/cm^2), and different incubation periods (4 h for calcium phosphate and 24 h for Effectene) to monitor the transfection performance under each condition by assaying the luciferase reporter gene activity. An additional parameter (*i.e.* different ratios of plasmid DNA to Effectene, ranging between 1:10 and 1:25 were tested) was also assessed for transfection efficiency using Effectene. Transfection efficiency was determined by counting cells (at least 600 cells randomly in four randomly selected fields, ~150 cells/field, under the microscope) with positive signals using either fluorescence microscopy (for pTracer-CMV2 which contains a green fluorescent protein reporter) or immunohistochemistry staining of TGF-β3 (for pCIneo), because non-TGF-β3-transfected Sertoli cells had relatively weak signals (see Fig. 1*B*). It is noted that counting transfected cells with positive signals (*e.g.* β-galactosidase or green fluorescent protein) is a common approach to determine transfection efficiency (17, 18). The integrity of the Sertoli cell TJ permeability barrier and its changes following transient transfection of TGF-β3 *versus* various controls were estimated by quantifying the transepithelial electrical resistance (TER) across the Sertoli cell epithelium when cells were cultured on Matrigel-coated bicameral units as earlier described (11).

Transient Disruption of BTB Induced by Local Administration of TGF-β3; an in Vivo Model for Studying BTB Dynamics—Groups of rats (~260–300 g body weight, $n = 3–4$ per time point for each experiment, with a total of four experiments conducted over a period of 2 years) received human recombinant TGF-β3 (catalog number PF073, Calbiochem) at 200 ng of TGF-β3/testis (single dose, with a mean ± S.D. testis weight of about 1.65 ± 0.15 g per testis, $n = 12$) (regimen 1). Preliminary experiments included administration of 80, 100, and 400 ng of recombinant TGF-β3/testis for 1 or 2 doses ($q - 1$ week) ($n = 2–3$ rats per time point), because results obtained from regimen 1 yielded clearly distinguishable and reversible damage at the BTB; results reported herein were representative data of these four experiments. This dosing of 200 ng of recombinant TGF-β3/rat testis that was selected is within the physiological range of TGF-β3 found in the adult rat testis. The physiological level of TGF-β3 in normal rat testes was estimated by immunoblot analysis as follows. Testis protein lysates at 100, 200, and 300 μg of total protein per lane were fractionated along with recombinant TGF-β3 at 1, 3, 5, 8, and 10 ng of protein per lane by SDS-PAGE (all samples in duplicate). The resultant blot was immunostained with an anti-TGF-β3 antibody, and TGF-β3 was visualized using an ECL kit (Amersham Biosciences). Thereafter, the primary and secondary antibodies in this blot were stripped in a stripping buffer (62.5 mM Tris-HCl, pH 6.8, at 22 °C, containing 100 mM 20-mercaptoethanol, 2% SDS (w/v), for 30 min in a reciprocating water bath, 40 rpm, at 55 °C), re-blocked with 6% milk (w/v), and then re-probed with an anti-actin antibody to assess equal protein loading. Protein bands corresponding to TGF-β3 and β-actin were scanned, and data were normalized against β-actin that served as a protein loading control. The amount of TGF-β3 in testis lysates was then interpolated from the resultant standard curve using different amounts of recombinant TGF-β3 (see above) by linear regression, plotting the area under the protein bands against protein levels. This analysis had shown that each adult rat testis contained about 1.1 ± 0.2 μg of TGF-β3 ($n = 4$). For *in vivo* administration, TGF-β3 was resuspended and solubilized in 4 mM HCl containing 0.1% bovine serum albumin (w/v). Just prior to its use, it was diluted in PBS (10 mM sodium phosphate, 0.15 M NaCl, pH 7.4, at 22 °C) at 1:10 to a final concentration of 1 ng/μl, and administered to two different sites (about 100 μl per site, see Fig. 3*A*, *inset*, for approximate location in the testis) intratesticularly using a 27-gauge needle as described previously (19, 20), which is a widely used methodology to assess effects of toxicants in the testis.

TABLE 2
The sources of different antibodies and their working dilutions used for different experiments in this report

Vendor	Target protein	Animal source[a]	Catalog no.	Lot no.	Usage[b]	Working dilution
Santa Cruz Biotechnologies	N-cadherin	Rabbit	sc-7939	J1502	IB	1:200
					IP	1:100
					IB	1:200
	β-Catenin	Rabbit	sc-7199	L0203	IF	1:100
					IP	1:100
	Nectin-3	Goat	sc-14806	K261	IB	1:200
	Actin	Goat	sc-1616	D052	IB	1:1000
	p-Smad2/3	Rabbit	sc-11769-R	E2303	IB	1:200
	TGF-β3	Rabbit	sc-82	H280	IB	1:200
					IHC	1:150
					IB	1:200
	TβR1	Rabbit	sc-398	E0305	IP	1:100
					IHC	1:150
	CD2AP	Rabbit	sc-9137	J1204	IB	1:200
	TAB1	Goat	sc-6052	L0904	IB	1:200
Cell Signaling	p-ERK (Thr^{202}/Tyr^{204})	Rabbit	9101S	13	IB	1:1000
	ERK	Rabbit	9102	10	IB	1:1000
	p-p38 MAPK (Thr^{180}/Tyr^{182})	Rabbit	9211	10	IB	1:1000
	p38 MAPK	Rabbit	9212	3	IB	1:1000
	JNK	Rabbit	9252	4	IB	1:200
	p-JNK	Mouse	9255	10	IB	1:200
Zymed Laboratories Inc.					IB	1:200
	Occludin	Rabbit	71–1500	30979485	IF	1:100
					IP	1:100
	N-cadherin	Mouse	33–3900	30778768	IF	1:100
	JAM-A	Rabbit	36–1700	30979650	IB	1:250
					IP	1:100
	ZO-1	Rabbit	61–7300	50799336	IB	1:150
					IP	1:100
	ZO-1	Mouse	33–9100	40890448	IF	1:100
BD Transduction Laboratories	Smad2/3	Mouse	610842	5	IB	1:500
Oncogene Research Products (San Diego)	Pan-Ras	Mouse	OP40	D20224-1	IB	1:250
R & D Systems (Minneapolis, MN)	TGF-β3	Goat	AF-243-NA	AAT01	IB	1:500

[a] All primary antibodies used in this report were polyclonal antibodies prepared in rabbits or goats or were monoclonal antibodies prepared in mice. These antibodies cross-reacted with the corresponding target proteins in rats.
[b] The abbreviations used are as follows: IB, immunoblotting; IP, immunoprecipitation; IF, immunofluorescence microscopy.

Vehicle controls referred to rats that received the same buffer containing no TGF-β3. All glassware and plasticware used to handle TGF-β3 were siliconized to minimize protein loss via nonspecific interactions. Rats were terminated at different checkpoints (*i.e.* time point at which a specific cellular event occurred) as follows: (i) time of TGF-β3 injection (time 0); (ii) time of appearance of BTB damage and germ cell loss (~4 h to 2 days); (iii) time of BTB recovery (~2–7 days); (iv) time of germ cell repopulation (~1–4 weeks); and (v) time of full recovery in which the seminiferous epithelium was indistinguishable from controls (~4 weeks). Controls included rats receiving the same volume of vehicle or PBS alone administered by the 27-gauge needle as described, or no treatment. As such, the BTB damage and the loss of Sertoli germ cell adhesion in the testis as reported here following TGF-β3 treatment are not the result of an artifact such as an increase in fluid pressure in the testis. Rats were terminated at specified time points by carbon dioxide asphyxiation, and testes were either frozen in liquid nitrogen or processed for paraffin sectioning. It is noted that the sites of TGF-β3 (or vehicle control) administration remained visible in testes for up to 2–4 weeks. As such, tissue blocks adjacent to these injection sites were cut (~0.1–0.2 g, which represented ~1/10 of the total testis) and were used for lysate preparation in an IP Lysis Buffer (see below). About 3–4 serial cross-sections from the three injection sites from each testis were used for both frozen (for fluorescent microscopy) and paraffin (for hematoxylin and eosin staining) sections.

Transient Disruption of Anchoring Junctions in the Seminiferous Epithelium without Compromising the BTB Integrity by Treating Rats with Adjudin [1-(2,4-dichlorobenzyl)-1H-indazole-3-carbohydrazide], an in Vivo Model for Studying AJ Dynamics—For rats that received adjudin to induce anchoring junction restructuring without compromising the BTB integrity (for review see Ref. 3), adult rats (~270–300 g, body weight) were treated with a single dose of adjudin at 50 mg/kg body weight by gavage as described (21). Adjudin was suspended in 0.25% methylcellulose (w/v with MilliQ water) at a concentration of 20 mg/ml. Rats in groups of ~3–5 were sacrificed at specified time points following treatment. Testes were immediately removed, frozen in liquid nitrogen, and stored at −80 °C until used. Control animals received vehicle control (*i.e.* the same volume of 0.25% methylcellulose suspended in water). Elongating and elongate spermatids began to deplete from the seminiferous epithelium by 8 h to 1 day after treatment, and ~50% of the round, elongating, and elongate spermatids, as well as spermatocytes, were depleted from the seminiferous epithelium in >90% of the tubules by day 4 (21). However, the Sertoli tight junctions at the BTB were shown to be unaffected during extensive anchoring junction restructuring that accompanied germ cell loss from the tubules (3, 22). Thus, this adjudin model was used to compare changes in the association between activated TβRI upon coupling with TGF-β3 and the adaptors CD2AP and TAB1 when only Sertoli germ cell anchoring junctions were reversibly disrupted without compromising the BTB integrity *versus* the TGF-β3 model when both BTB and AJ were disrupted.

Fluorescence, Light and Electron Microscopy, and Immunohistochemistry—Fluorescence microscopy using cross-sections of frozen testes (~6 μm thickness) to co-localize different integral membrane proteins (*e.g.* N-cadherin, occludin, and JAM-A) and adaptors (*e.g.* β-catenin, ZO-1) was performed essentially as described earlier (9, 15). To visualize Sertoli cells following overexpression with TGF-β3, cells grown on cover glass were fixed in methanol at −20 °C for 10 min, permeabilized with 0.2% Triton X-100 in PBS, blocked with 10% normal goat serum, and incubated with the corresponding primary antibody pairs (see Table 2). For light microscopy, paraffin sections (~6 μm thickness) were stained with hematoxylin and eosin. TGF-β3-treated

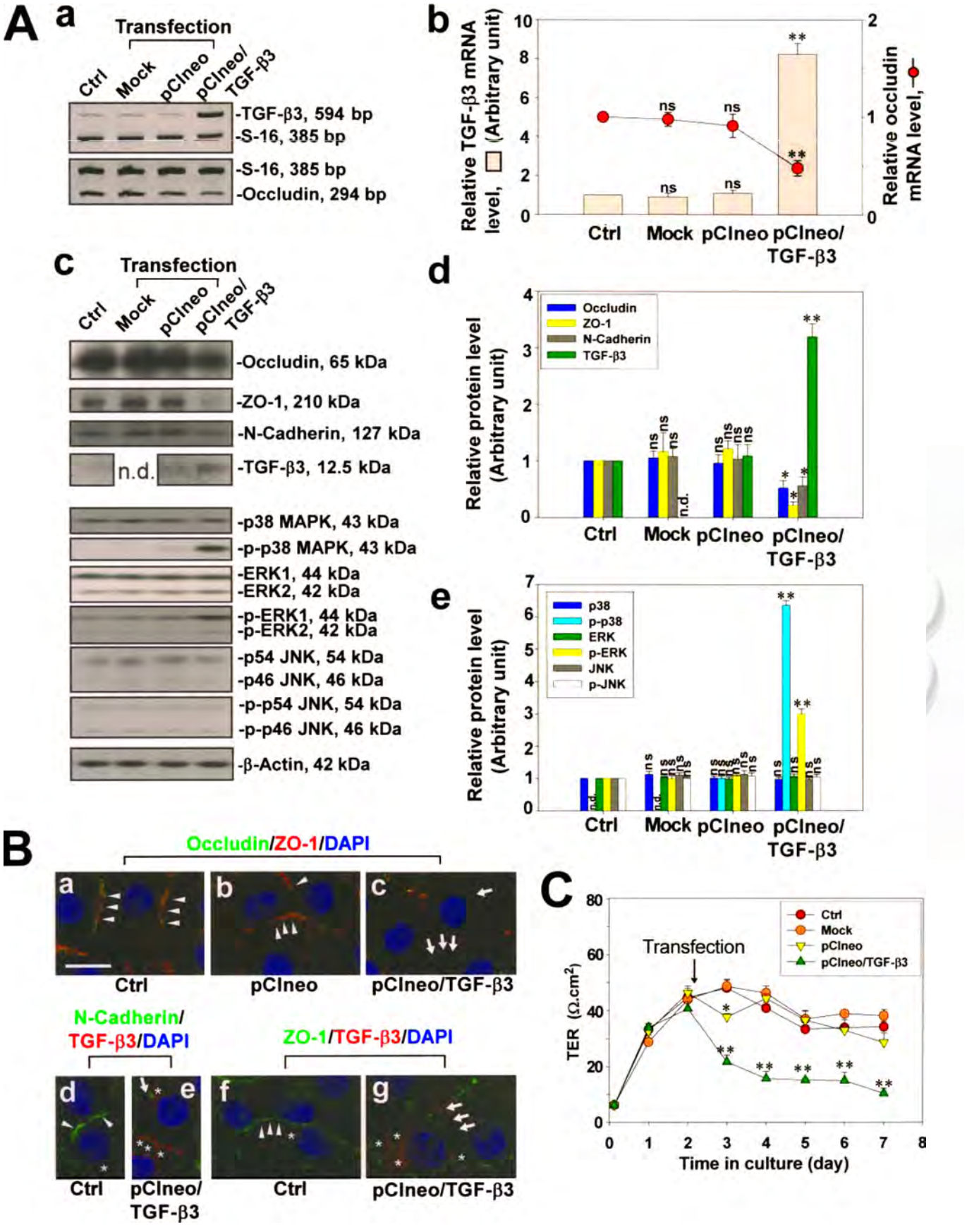

AQ: J FIGURE 1. **Overexpression of TGF-β3 in Sertoli cells cultured *in vitro* can perturb both TJ and AJ function.** *A, panels a–e,* RT-PCR (*panels a* and *b*) and immunoblot (*panels c–e*) analyses of primary Sertoli cells transiently transfected with a plasmid containing the TGF-β3 full-length cDNA (*pCIneo/TGF-β3*). Control (*Ctrl*), no treatment; *Mock*, transfection performed without the plasmid DNA; *pCIneo*, plasmid alone without TGF-β3 cDNA. The steady-state protein levels of occludin, ZO-1, N-cadherin, and TGF-β3 were compared

testes were examined, and ~150 seminiferous tubules were counted per testis in each experimental group by scoring a total of randomly selected tubules (~600 tubules total) for each time point from four testes. In brief, cross-sections of testes were placed under an Olympus BX40 microscope using a 10× objective, and 10 randomly selected fields were photographed using an Olympus DP70 and printed using an Epson 890 Inkjet printer. Damaged tubules were then scored and defined by those tubules with elongated spermatids ($n > 10$, except for stage IX tubules), round spermatids, and/or spermatocytes ($n \geq 5$) found in the tubule lumen as described (15). Changes in tubule diameters were also scored (16). The scoring of tubules was conducted by two separate investigators using coded slides, and results were analyzed and decoded by a third investigator to obtain unbiased composite data. Immunohistochemistry staining of TGF-β3 and TβR1 using frozen sections of testes (~7 μm in thickness) was performed essentially as described previously (15), and the antibody dilutions that were used for these experiments are shown in Table 2. Controls include sections incubated with normal rabbit IgG in stead of the primary antibody against TGF-β3. For all morphology studies, different samples within a treatment group *versus* controls were processed in a single experimental session using cross-sections of testes (~3–4 sections per glass slide) so that all sections were treated similarly, including primary and secondary antibodies and/or color development. Electron microscopy was performed at the Rockefeller University Bio-Imaging Facility (12). In brief, rats treated with 200 ng of TGF-β3 per testis or with vehicle control were terminated on day 2 by CO_2 asphyxiation. Testes were removed, incised to release the seminiferous tubules, and fixed in a 0.1 M sodium cacodylate buffer, pH 7.4, at 22 °C, containing 2.5% glutaraldehyde (v/v) for ~4 h, followed by post-fixation in OsO_4 (1%) and staining in 1% uranyl acetate. Tissues were dehydrated in ascending concentrations of ethanol, incubated in propylene oxide, and then infiltrated with EMbed (Electron Microscopy Sciences, Fort Washington, PA). Ultrathin sections (~80 nm thickness) were cut using a Reichert-Jung Ultracut E microtome (Bannockbum, IL) and post-stained with uranyl acetate/lead. Cross-sections of tubules were then examined and photographed on a JEOL 100CXII Electron Microscope (Peabody, CA) at 80 kV. Although only a representative set of experiments was reported here, all experiments were repeated at least three times (excluding preliminary experiments to select the appropriate antibody titers and primary/secondary antibody incubation conditions) using testes from different animals or Sertoli cells from different experiments, and similar results were obtained in these experiments.

RT-PCR, Immunoblottings, Co-immunoprecipitation (Co-IP), and Intrinsic p38 and ERK Assays—Semi-quantitative RT-PCR and immunoblottings were performed as described (11, 15). In selected experiments where Sertoli cells were transiently transfected with the full-length TGF-β3 cDNA, the steady-state levels of total p38 MAPK, ERK1/2, the JNK *versus* the corresponding activated (phosphorylated) were also estimated by immunoblottings to monitor if any of these downstream signal transducers were being activated. Cell lysates were obtained by solubilizing proteins from Sertoli cells cultured in 6-well dishes (in triplicate) using lysis buffer (10 mM Tris, pH 7.4, at 22 °C, containing 1% SDS (w/v), 1.6 2-mercaptoethanol, 1 mM EGTA, 2 mM phenylmethylsulfonyl fluoride, 2 mM *N*-ethylmaleimide) (10 min at room temperature, followed by centrifugation at 15,000 × *g* for 15 min at 4 °C to obtain the clear supernatant that served as the lysate). Co-IP was performed as detailed elsewhere (9). In brief, testis lysates (~500 μg of protein per sample) prepared in an IP Lysis Buffer (10 mM Tris, pH 7.4, at 22 °C, containing 0.15 M NaCl, 2 mM phenylmethylsulfonyl fluoride, 1 mM EGTA, 1% Nonidet P-40 (v/v), 1 mM sodium orthovanadate, 1 μg/ml leupeptin, 1 μg/ml aprotinin, and 10% glycerol (v/v)) from each sample was used for Co-IP. Equal amounts of testis lysates (~125 μg of protein/sample) estimated by Coomassie Blue dye-binding assay (23) or extracted immunocomplexes from Co-IP experiments were used for immunoblottings and probed for different target proteins (see Table 2). Intrinsic ERK and p38 MAPK assays were performed using specific p-ERK and p38 MAPK assay kits (Cell Signaling) with the corresponding fusion proteins Elk-1 and ATF-2. The corresponding activated (phosphorylated) transcription factors, namely p-Elk-1 and p-ATF-2, were visualized by immunoblottings using specific antibodies provided in the kits. Proteins were visualized by using chemiluminescence kits obtained from Amersham Biosciences. Each experiment was repeated at least three times using data from different animals. All samples within an experimental group were processed simultaneously in an experimental session to eliminate inter-experimental variations. Data were densitometrically scanned using SigmaGel (version 3.0) from SPSS Inc.

Image and Statistical Analyses—Gel images from RT-PCR and immunoblots were scanned using SigmaGel software (SPSS Inc., version 1.05). One-way ANOVA to be followed by the Tukey's honestly significant test was performed using the JMP IN statistical analysis software package (version 4; SAS Inc., Cary, NC).

RESULTS

Overexpression of TGF-β3 in Sertoli Cells Disrupted Both TJ and AJ Integrity in Vitro

Primary Sertoli cells cultured *in vitro* were transfected with plasmids containing the full-length TGF-β3 (pCIneo/TGF-β3) with ~15% efficiency. About 24 h after transfection, both the steady-state mRNA (Fig. 1, *A, panels a,* and *b*) and protein levels of TGF-β3 increased significantly (Fig. 1, *A, panels c* and *d*), concomitant with a significant reduction in occludin, ZO-1, and N-cadherin (Fig. 1*A, panels a--d*), suggesting both the TJ and AJ function were perturbed. Overexpression of TGF-β3 in Sertoli cells, but not with empty vector, was also shown to induce activation (*i.e.* phosphorylation) of p38 and ERK MAP kinases but not JNK (Fig. 1, *A, panels c* and *e*). These results are also consistent with recent *in vitro* and *in vivo* findings investigating the regulatory roles of TGF-β3 on BTB dynamics (15, 24). As shown in Fig. 1*B, panel a*, intact TJ fibrils formed in part by occludin (*green*) and its adaptor ZO-1 (*red*) was detected and co-localized at the Sertoli interface. Transfection of Sertoli cells with pCIneo/TGF-β3, however, not only reduced the protein levels of occludin and ZO-1 at the cell-cell interface but also caused significant disruption of the immunoreactive "belt-like" structure, an indication of broken TJs between Sertoli cells. This effect was not seen in cells transfected with empty vector (Fig. 1, *B, panel c versus panel b*). Likewise, overexpression of TGF-β3 (*red fluorescence* in Fig. 1*B, panel e*) also affected N-cadherin and ZO-1 levels and their distribution *versus* control (Fig. 1*B,* compare *panels d* and *f* with *e* and *g*). Furthermore, we monitored the effects of TGF-β3 overexpression in

AQ: E

F1

(*panels c* and *d*). The steady-state protein levels of p38, ERK, and JNK MAP kinases, and their corresponding activated (*i.e.* phosphorylated) forms in cells with transient transfection of TGF-β3 cDNA *versus* other controls were also assessed (*panel e*). β-Actin served as a protein loading control. *B,* fluorescent micrographs of Sertoli cells transfected with pCIneo/TGF-β3 *versus* control and pCIneo alone. Cells were stained with different target proteins (*e.g.* occludin, N-cadherin, and ZO-1) and TGF-β3. *White arrowheads* depict the TJ or basal ES site where protein(s) formed an intact belt-like barrier between neighboring Sertoli cells; *white arrows* indicate the disrupted TJ barrier, manifested by the broken belt-like structures; *asterisks* indicate TGF-β3 staining. *C,* TER of Sertoli cells cultured in bicameral units that were transfected with pCI-neo/TGF-β3 *versus* controls. Each data point is the mean ± S.D. of three experiments. *ns*, not significantly different by ANOVA; *, $p < 0.05$; **, $p < 0.01$; *n.d.*, not detectable.

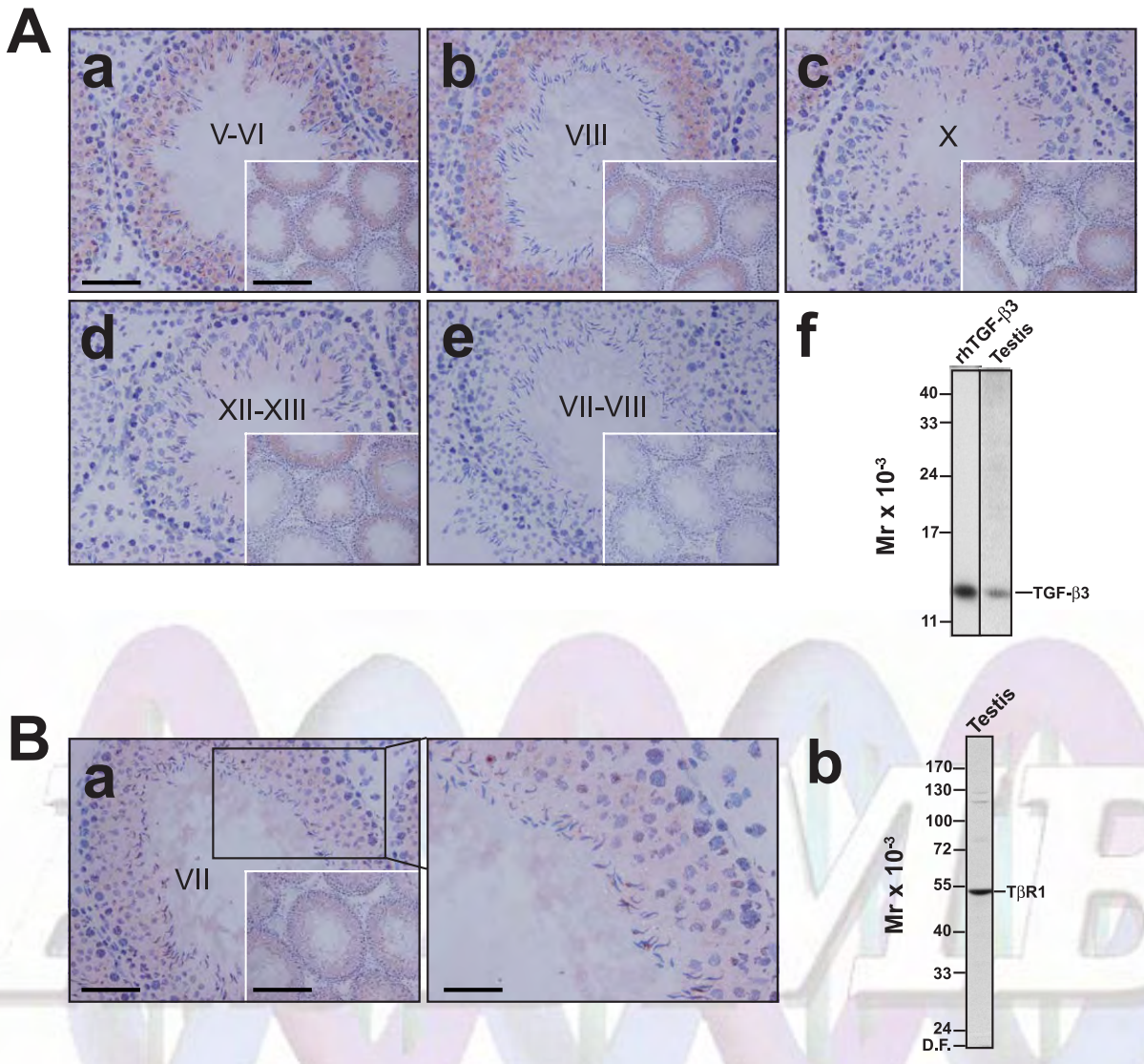

FIGURE 2. **A study to examine the localization and stage specificity of TGF-β3 and TβR1 in the seminiferous epithelium of adult rat testes by immunohistochemistry.** Frozen sections (7 μm in thickness) of testes from adult rats (~300 g body weight) and an antibody against either TGF-β3 (*A*) or TβR1 (*B*) (see Table 2) were used for immunohistochemistry using procedures as described (9). *A,* TGF-β3 was predominant at stages V–VIII tubules; its staining was reduced at stages X–XIII (see *panels a* and *b versus panels c* and *d*, including *insets* showing the lower magnifications of the corresponding micrographs). At stages VII and VIII, intense staining of TGF-β3 in the epithelium as shown in *panel b* (see also *inset* to *panel b*) is consistent with its localization at the BTB. *Panel e*, this is a control section stained with normal rabbit IgG, illustrating the staining shown in *panels a–d* is specific for TGF-β3. In *panel f*, this is an immunoblot using 5 ng of recombinant human TGF-β3 and 100 μg of protein of testis lysate and stained with the anti-TGF-β3 antibody, illustrating the specificity of this antibody. *Bar* in *panel a* = 50 μm; *bar* in *inset* = 200 μm, which also applies to *panels b–e*. Because an increase in TGB-β3 staining as reported here and elsewhere (15, 24) was not just associated with stages VII–VIII tubules, we speculate that its increase in the epithelium at stages V–VI may have other physiological functions, plausibly unrelated to preleptotene/leptotene spermatocyte migration across the BTB that occur at VII–VIII. This is not entirely unexpected because TGF-β3 affects multiple testicular function (14, 33). *B,* these micrographs illustrate the immunohistochemical localization of TβR1 in the seminiferous epithelium of adult rat testes. TβR1 did not display the same stage specificity as of TGF-β3 (see *panel a* in *B versus panels a–f* in *A*). Instead, TβR1 was detected in the epithelium in almost all stages of the epithelial cycle, but it was found at the site consistent with its localization at the BTB (see the *right panel* in *panel a*, which is the magnified view of *panel a*). In *panel b*, this is an immunoblot using 100 μg of protein of adult rat testis lysate stained with the anti-TβR1 antibody, illustrating the specificity of the antibody. *Bar* in *panel a* = 50 μm; *bar* in *inset* = 200 μm; *bar* in *right panel* = 25 μm; *D.F.*, dye-front.

Sertoli cells on the TJ barrier functionally by quantifying the TER across the Sertoli cell epithelium on Matrigel-coated bicameral units (Fig. 1*C*). Transient transfection was performed on day 2 when Sertoli cells had formed a functional TJ barrier (11, 16). Consistent with results by immunoblottings and fluorescence microscopy, overexpression of TGF-β3 indeed disrupted the TJ permeability barrier by reducing TER by ~2-fold *versus* controls (15–20 ohms·cm^2 *versus* 35–40 ohms·cm^2 in controls) (Fig. 1*C*).

TGF-β3 and TβR1 Expression in the Seminiferous Epithelium

It is known that TGF-βs are multifunctional molecules that affect numerous testicular function, including steroidogenesis, cell differentiation, and germ cell development (for a review see Ref. 14). It is conceivable that if TGF-β3 indeed plays a crucial role in regulating BTB dynamics *in vivo*, TGF-β3 and its receptor should reside close to the BTB. Furthermore, its expression should be peaked in the seminiferous epithelium at stages VII–VIII when preleptotene and leptotene spermatocytes are traversing the BTB. Although an early study reported the enhanced expression of TGF-β3 at stage VII–VIII (24), its pattern of localization in the seminiferous epithelium of a stage VIII tubule was not shown. We have thus performed a detailed immunohistochemistry analysis as shown in Fig. 2. Consistent with this earlier study (24), TGF-β3 was found to be highly expressed in stages V–VIII tubules; however, its staining was greatly reduced at stages X–XIII (see Fig. 2*A*, *panels a* and *b versus c* and *d*, including *insets* in the micrographs, which are the lower magnifications of the corresponding micrographs show-

balt3/zbc-bc/zbc-bc/zbc02506/zbc5559-06g saylora S=3 2/5/06 15:18 **4/Color Figure(s) F1–3,6,8** ARTNO: M601618200

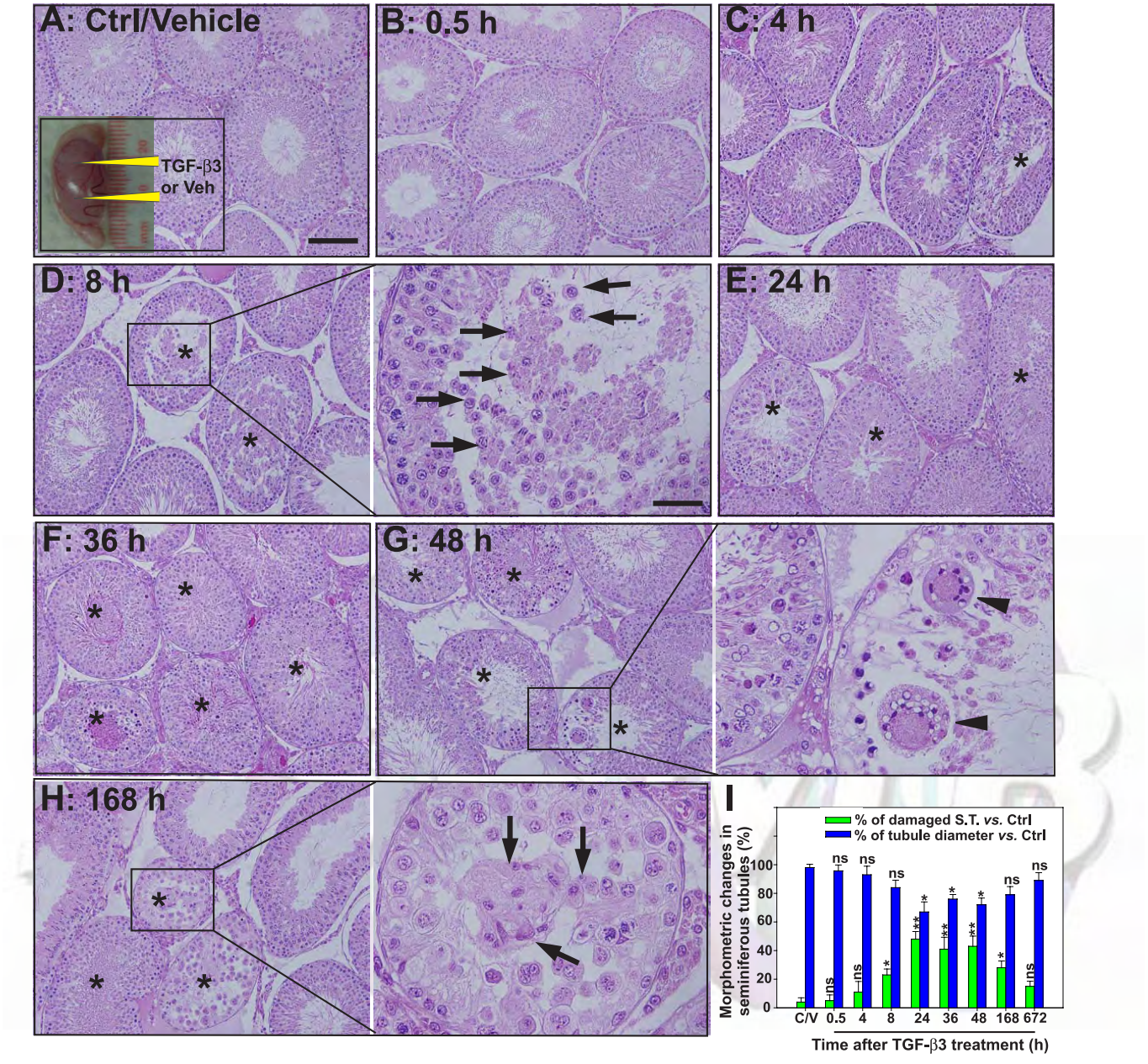

FIGURE 3. **Effects of local administration of TGF-β3 to rat testes on the status of spermatogenesis and the kinetics of germ cell loss from the epithelium.** *A,* recombinant TGF-β3 or vehicle (*Veh*) was injected into the testis using a 27-gauge needle at ~2 sites/testis (see *yellow arrowheads*) at time 0 (*i.e. Ctrl*, control) (see *inset* to *A*). The weight of testes did not alter during the treatment (data not shown). *B–H,* representative photographs of paraffin sections stained with hematoxylin and eosin from testes treated with TGF-β3 at specified time points; the vehicle control is shown in *A*. Morphometric changes (% of tubules with germ cell exfoliation and shrinkage of tubule diameter) of the tubules are summarized in the bar graph shown in *I*. *Asterisk* indicate tubules with notable germ cell loss; *arrows* indicate germ cells, such as spermatocytes and round spermatids, and were found in the tubule lumen; *arrowheads* indicate multinucleated germ cells, an indication of either necrosis or a collapse of germ cell syncytium that occurs prior to apoptosis. *Bar* = 120 μm in *A* and applies to all graphs except for the magnified views of the corresponding *boxed areas* where *bar* = 40 μm. *ns*, not significantly different by ANOVA; *, $p < 0.05$; **, $p < 0.01$.

ing more staged tubules). At stages VII and VIII, the intense staining of TGF-β3 in the seminiferous epithelium as shown in Fig. 2*A*, *panel b* (see also *inset* to *panel b*), is consistent with its localization at the BTB near the basal lamina. Significant amounts of immunoreactive TGF-β3 was also detected in the seminiferous epithelium and was associated with round spermatids (see Fig. 2*A*, *panels a–d*). This is not entirely unexpected because TGF-β3 was shown to have other physiological functions in the testis (*e.g.* germ cell development) (for reviews see Refs. 14 and 25) other than its involvement in BTB dynamics as reported here. In Fig. 2*A*, *panel e*, this is the section stained with the normal rabbit IgG, illustrating the staining shown in *panels a–d* is specific for TGF-β3. In Fig. 2*A*, *panel f*, this is an immunoblot using recombinant human TGF-β3 and testis protein lysate and is stained with the anti-TGF-β3 antibody, illustrating the specificity of this antibody. Fig. 2*B* illustrates the immunohistochemical localization of TβR1 in the seminiferous epithelium of adult rat testes. Interestingly, TβR1 did not display the same stage specificity as of TGF-β3 (see a in Fig. 2*B versus a–f* in *A*). Instead, TβR1 was detected in the seminiferous epithelium in almost all stages of the epithelial cycle, but it was also found at the site consistent with its localization at the BTB (see the *right panel* in Fig. 2*B*, *panel a*, which is the magnified view of the *boxed area* in *a*). The results shown in Fig. 2*B* did not negate the significance of the stage-specific induction of TGF-β3 detected in stages V–VIII as shown in Fig. 2*A*; in contrast, they

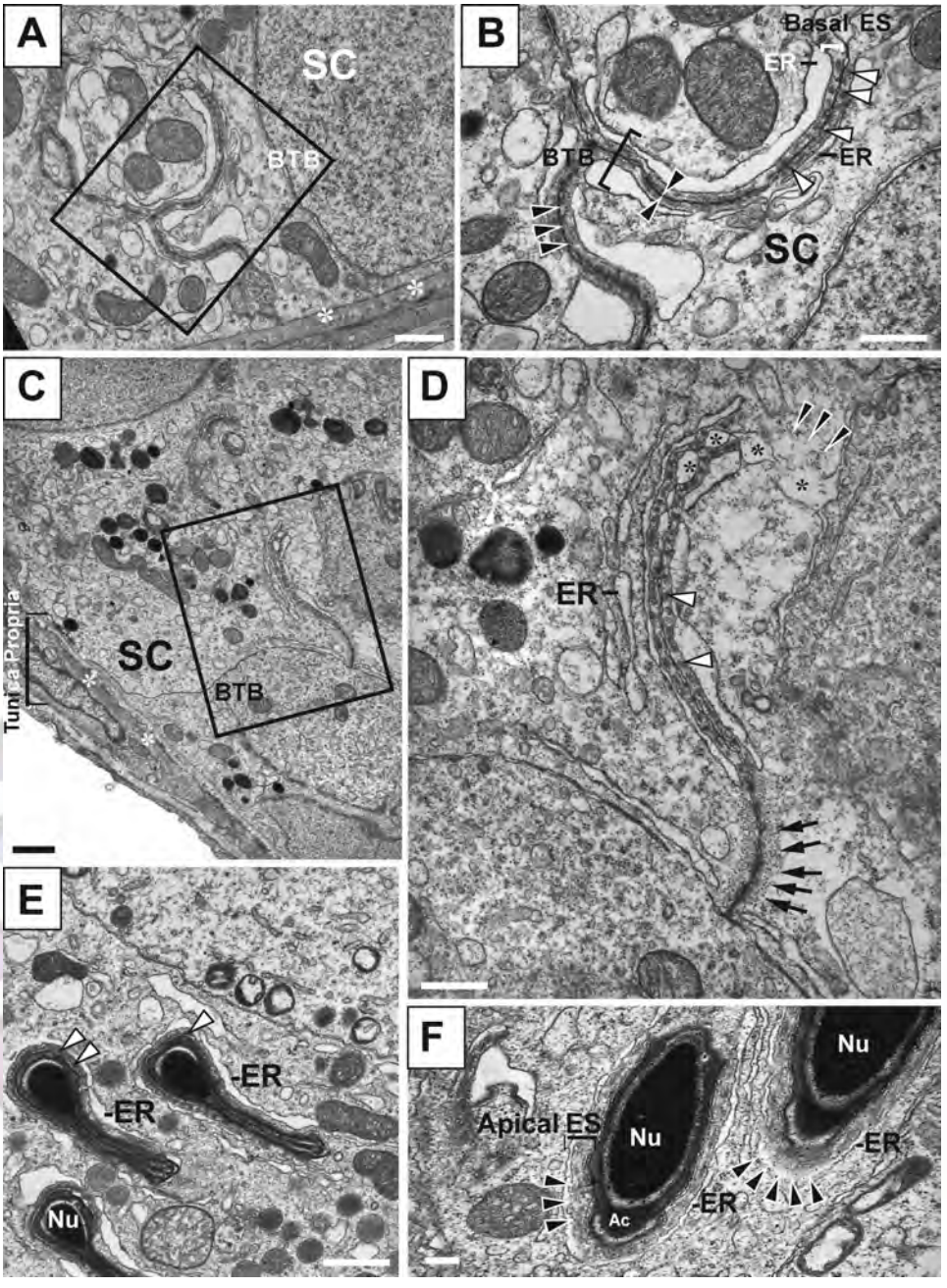

FIGURE 4. **Ultrastructural changes in the testis on day 2 after treatment with TGF-β3 (200 ng/testis), *A*, *B*, and *E* indicate vehicle controls; *C*, *D*, and *F* indicate treatment group.** *A* and *B*, the cross-section of a normal seminiferous tubule from adult rat testes showing the epithelium lying on the basement membrane (*white asterisks*) and the BTB (*boxed area*) was magnified and is shown in *B*. BTB is composed of TJ (*black arrowheads*) coexisting with basal ES, which is typified by the presence of actin bundles (*white arrowhead*) sandwiched between cisternae of endoplasmic reticulum (*ER*) and Sertoli cell (*SC*) membrane that is clearly visible on both sides of the Sertoli cells (apposing *black arrowheads* represent two apposing SC membranes). *C* and *D*, the BTB in TGF-β3-treated testes displayed obvious structural damages in which the ER and the actin filament bundles were dissolving (see *black arrowheads*) with the presence of swelling intercellular space between the two SCs (see *asterisks*). *E*, typical apical ES in the seminiferous epithelium of normal rats between elongating spermatids (*Nu*, nucleus) and SC in which actin bundles (*white arrowheads*) sandwiched between SC membrane and ER and restricted to the SC. *F*, both actin bundles and ER were defragmented, disappearing from the apical ES (*black arrowhead*) in TGF-β3 treated testis. *Ac*, acrosome. *Bar: A*, 0.5 μm; *B*, *D*, and *F*, 0.2 μm; *C* and *E*, 1 μm.

reinforce the notion as described above that TGF-β3 is crucial to other seminiferous epithelial function in addition to BTB dynamics. In Fig. 2*B*, *panel b*, this is an immunoblot using adult rat testis protein lysate stained with the anti-TβR1 antibody, illustrating the specificity of the antibody used for immunohistochemistry shown in Fig. 2*B*. In short, these experiments illustrate that TGF-β3 and its receptor, TβR1, are present at the BTB site, and the stage-specific expressions of TGF-β3 in the epithelium are consistent with their involvement in BTB dynamics.

An in Vivo Model for Studying BTB and AJ Dynamics

Changes in the Status of Spermatogenesis following TGF-β3 Treatment—To test if local administration of TGF-β3 reversibly perturbed the BTB *in vivo*, TGF-β3 (200 ng/testis) was administered to the testis via intratesticular injection at two sites (see Fig. 3*A*, *inset*). Although this treatment did not elicit any significant changes in testis weight over the 4-week experiment period (data not shown), histological analysis of these testes revealed that TGF-β3 caused germ cell depletion from the epithelium, which was limited to elongate/elongating/round spermatids and some late spermatocytes (Fig. 3, *A–H*). This disruptive effect on Sertoli germ cell interface was not detected by 30 min post-treatment, but some signs of damage were visible by 4 h; this effect was most prominent at 24–48 h when the damaged tubules were ~40% in the epithelium, and the tubule diameters shrunk by ~20% (Fig. 3, *C–G versus A* and *B*). This damaging effect began to recede by 1 week (Fig. 3*H*), and by 4 weeks most of the tubules (>97%) were indistinguishable from controls (Fig. 3*I*). This time frame of germ cell depletion following TGF-β3 treatment and their repopulation in the epithelium also suggests that most of the spermatocytes were not affected so that they can repopulate the seminiferous epithelium within ~20 days, consistent with the micrographs shown in Fig. 3. In this context, it is of interest to note that the phagocytic

F3

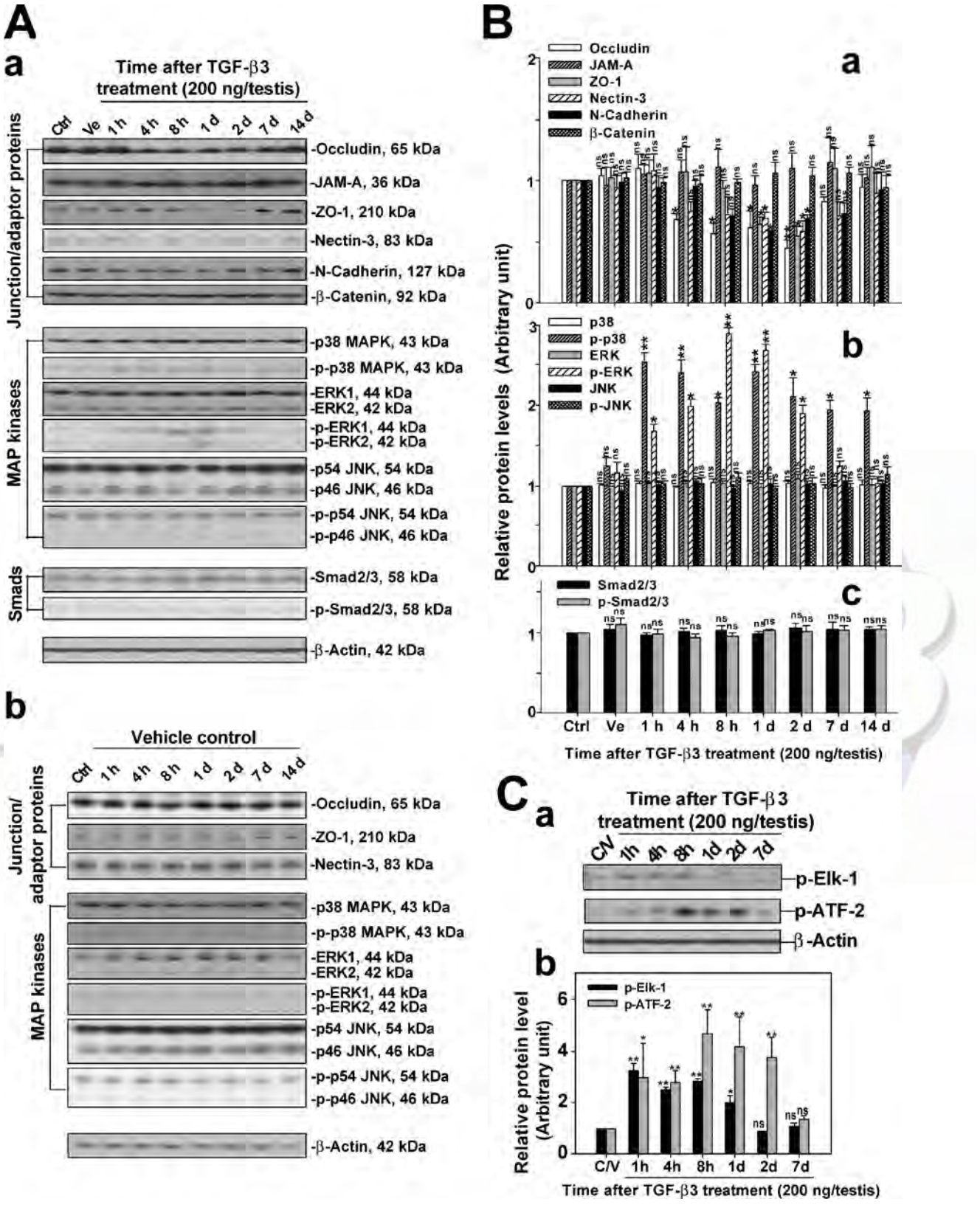

FIGURE 5. **Changes in different target proteins, including MAP kinases in testes during TGF-β3-induced BTB and AJ disruption in the testis.** *A,* immunoblot analysis to assess the changes of protein levels after TGF-β3 treatment in the rat testis. These include the representative integral junction membrane proteins and their adaptors at the BTB and apical ES, the three MAP kinases, and Smad2/3 and their corresponding phosphorylated (activated) forms (*panel a*). Parallel immunoblot analysis of these proteins in the testes of adult rats received vehicle control (*panel b*). *B,* densitometric scanned data of immunoblots such as those shown in *A*. Each *bar* is the mean ± S.D. of three independents sets of samples from different experiments. *C,* intrinsic kinase activity of ERK (substrate, Elk-1) and p38 (substrate, ATF-2) (*left panel*), and these data were also summarized in the *right panel* ($n = 3$). *ns*, not significantly different by ANOVA; *, $p < 0.05$; **, $p < 0.01$; *h*, hour; *d*, day.

activity of Sertoli cells appeared to be activated by TGF-β3 treatment as shown in Fig. 3, which is likely the result of an increase in germ cell necrosis as shown by the multinucleated cells seen here (*e.g.* Fig. 3, *F* and *H*). At present, it is not known if an increase in phagocytosis is associated with the transient BTB disruption.

Ultrastructural Changes at the BTB following TGF-β3 Treatment—The ultrastructural changes after TGF-β3 treatment were also examined by electron microscopy and are shown in Fig. 4. In normal testes, BTB that was composed of co-existing TJ and basal ES was readily visible (see *boxed area* in Fig. 4*A*, which is magnified in Fig. 4*B*). Basal ES was typified by the presence of actin bundles (*white arrowheads* in Fig. 4) sandwiched between apposing Sertoli cell membranes (apposing *black arrowheads*) and the cisternae of the endoplasmic reticulum (ER), coexisting with TJ (*black arrowheads*) at the BTB (Fig. 4*B*). However, by 2 days after TGF-β3 treatment (200 ng/testis), the voided intercellular space was frequently found between apposing Sertoli cell membranes at the BTB (*black asterisks*), coupled with defragmentation of actin bundles (*black arrows*) (Fig. 4, *C* and *D*), illustrating a disruption of the BTB. Apical ES between spermatids and Sertoli cells, a structure similar to basal ES but the actin filament bundles and the cisternae of ER were found only on the Sertoli cell side, was also found to be disrupted after TGF-β3 treatment (Fig. 4, *F versus E*). For instance, the actin bundles at the apical ES in normal testes (see *white arrowheads* in Fig. 4*E*) were found to become extensively disorganized with the simultaneous loss of the ER at the apical ES (*black arrowheads* in Fig. 4*F*). These results illustrate that TGF-β3, when administered locally, was capable of disrupting both TJ and basal ES at the BTB and apical ES.

Changes in Target Protein Levels in the Seminiferous Epithelium and Intrinsic Kinase Activities of p38 and ERK MAPK during TGF-β3-induced BTB and AJ Damage—By using immunoblottings, the steady-state levels of target junction junctions/adaptors at the BTB and ES were analyzed (Fig. 5). The occludin level was significantly reduced between 4 h and 1 week, being most severe at 1–2 days to ~50% of control (Fig. 5, *A* and *B*). By 1–2 days, the ZO-1 level was also reduced significantly (Fig. 5). JAM-A, another TJ integral membrane protein in the testis, however, was unaffected (Fig. 5). There was also a decline in N-cadherin and nectin-3 (an AJ protein restricted to spermatids (26)) but not the adaptor protein β-catenin (Fig. 5). Furthermore, TGF-β3 activated both the ERK and p38 MAPK signal transducers but not JNK or Smad2/3. These observations appeared to be specific to the TGF-β3 treatment because testes from rats treated with vehicle alone (see "Experimental Procedures") exhibited no changes in the levels of these junction/adaptor proteins nor phosphorylation of any three MAP kinases (Fig. 5*A*, *panel b*) An activation of p-ERK and p38 MAPK was further confirmed by specific intrinsic kinase assays for the corresponding MAPKs during TGF-β3-induced BTB and AJ disruption because the putative substrates, namely transcription factors p-Elk-1 and p-ATF-2, specific for p-ERK and p38, respectively, were indeed significantly induced by TGF-β3 treatment (Fig. 5*C*).

Reversible BTB Damage after TGF-β3 Treatment—We next examined the distribution of occludin/ZO-1 (Fig. 6*A*), N-cadherin/β-catenin (Fig. 6*B*), and JAM-A/ZO-1 (Fig. 6*C*) in testes from rats by 2 days and 2 weeks after TGF-β3 treatment *versus* control testis using fluorescence microscopy to monitor the BTB integrity (Fig. 6). In normal testes, occludin, JAM-A, and N-cadherin were localized with their adaptors ZO-1 and β-catenin at the basal compartment of the seminiferous epithelium, consistent with their localization at the BTB (Fig. 6, *A–C*). More importantly, this loss of occludin, ZO-1, and N-cadherin, but not β-catenin, from the epithelium was transient (Fig. 6, *A* and *B*), because by week 2 these proteins were found to localize at the BTB site virtually indistinguishable from control testes (Fig. 6, *A, panels i--l,* and *B, panels i--l*) and consistent with the results of immunoblottings (Fig. 6 *versus* Fig. 5). It must be noted that this technique, when used in conjunction with immunoblottings, is a powerful tool to accurately monitor BTB integrity, and is indistinguishable from the more tedious techniques, such as micropuncture, to quantify the diffusion of ^{125}I-labeled bovine serum albumin from the system circulation to rete testis and seminiferous tubule fluids to assess BTB integrity (12, 27).

The Activated TGFβ3-TβR1 Complex Recruits Either Adaptors CD2AP and TAB1 or CD2AP Alone to the BTB to Selectively Activate Different MAPK Signal Transducers

When TGF-β3 binds to its receptors (type II, TβRII, and type I, TβR1), the ligand-receptor complex, in turn, recruits different adaptors to phosphorylate selective downstream kinases, leading to an activation of distinct MAP kinase(s), thereby regulating different physiological events (14, 28, 29). As shown in Fig. 7*A*, adaptors CD2AP and TAB1 were indeed expressed by both Sertoli and germ cells even though they are not uniformly distributed in these two cell types (Fig. 7*A*). Furthermore, CD2AP was shown to associate with N-cadherin, β-catenin, ZO-1, and JAM-A, but not occludin, in lysates of normal seminiferous tubules, unlike TAB1 which was shown to associate with all these proteins (Fig. 7*B*). Results shown in Fig. 7*B* were consistent with recent observations that CD2AP was localized predominantly to the basal compartment at the BTB in rat testes by immunohistochemistry[3] and in mouse testes (30), co-existing with N-cadherin, β-catenin, ZO-1, and JAM-A (9, 15). In adjudin-treated rat testes, it was shown that the loss of germ cells from the epithelium was associated with a transient TGF-β3 induction, and an activation of ERK but not p38 MAPK, which led to AJ disruption and germ cell loss from the epithelium without compromising the BTB integrity (15). As such, these two models, namely the TGF-β3 and adjudin models, provide the means to identify the intriguing protein-protein associations between TGF-β3/TβR1 and TAB1 and/or CD2AP when both BTB and Sertoli germ cell adhesion (the TGF-β3 model) or only Sertoli germ cell adhesion (the Adjudin model) was perturbed. When samples from both models were analyzed simultaneously in a single experimental session to eliminate inter-experimental variation and as shown in Fig. 7, *C–F*, it was noted that by using an anti-TβR1 antibody as the precipitating antibody, it could pull out significantly more CD2AP and TAB1 as well as Ras GTPase by 4 h to 1 day when the BTB and Sertoli germ cell adhesion was disrupted in the TGF-β3 model, whereas the level of TβRI *per se* remained relatively constant (Fig. 7*C*). When the lysates from these samples were examined by immunoblottings and compared with Co-IP data (*right panel versus middle panel* in Fig. 7*C*), it was noted that the relative protein levels of CD2AP, Ras, and TβRI did not change with TGF-β3 treatment except that TAB1 was induced ~2-fold by 4 h (see Fig. 7*D*), but there was an increase in the association between TβRI and adaptors CD2AP and TAB1 at the time of BTB *and* Sertoli germ cell adhesion disruption (Fig. 7, *C* and *D*). By using samples from the adjudin model when only Sertoli germ adhesion was disrupted without perturbing the BTB integrity (3), it was noted that there was a significant increase in the protein-protein association between TβRI and CD2AP and Ras GTPase by 8 h and 1 day post-treatment, but an ~2–3-fold decline in association between TβRI and TAB1 by 1 and 4 days (see Fig. 7, *E* and *F*). However, the

[3] W. Xia and C. Y. Cheng, unpublished observations.

balt3/zbc-bc/zbc02506/zbc5559-06g saylora S=3 2/5/06 15:18 4/Color Figure(s) F1–3,6,8 ARTNO: M601618200

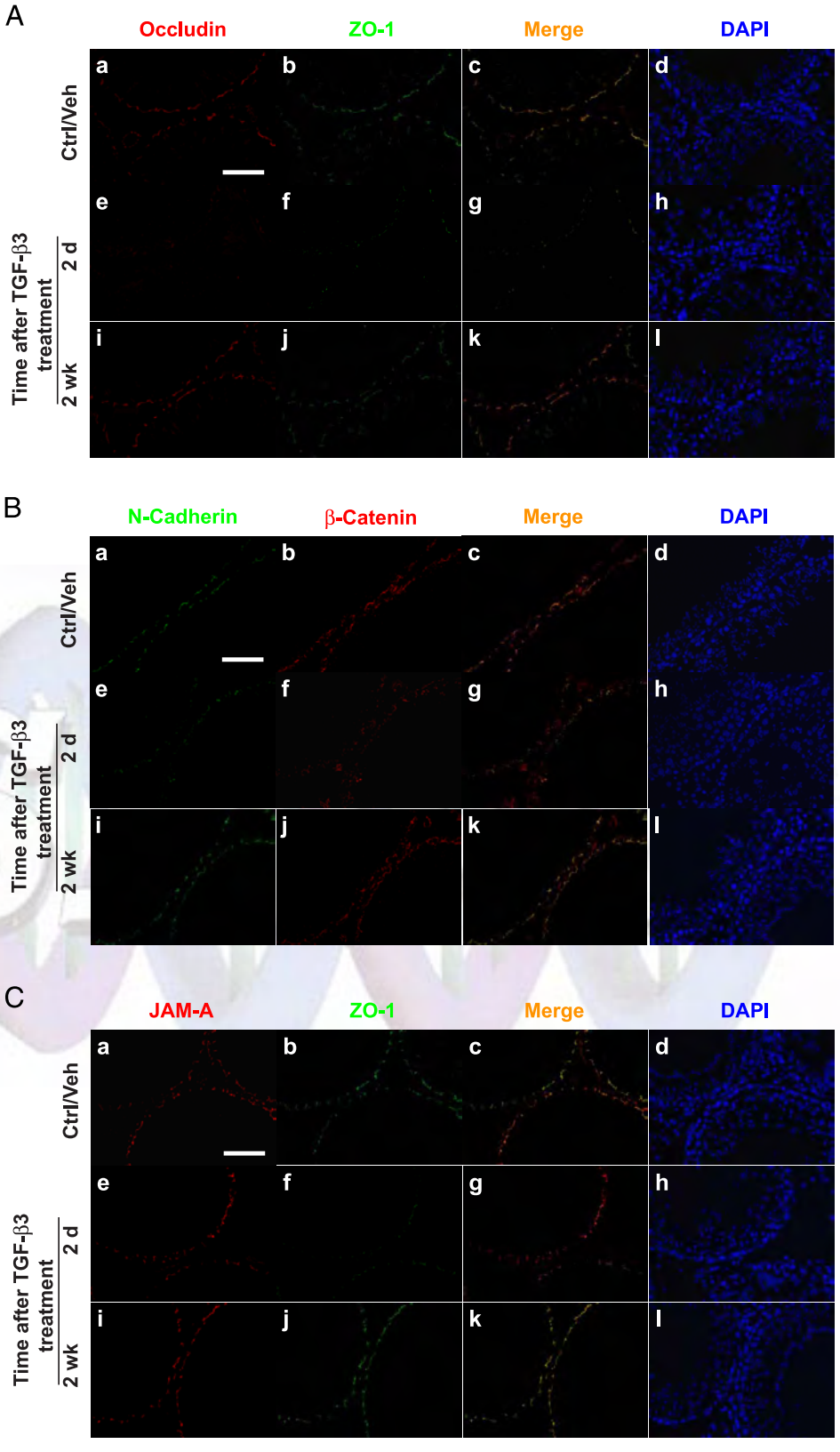

FIGURE 6. **A study to assess the reversibility of the TGF-β3-induced BTB damage by fluorescence microscopy.** Cryosections (~7 μm) of testes from vehicle control, 2 days and 2 weeks after TGF-β3 treatment, were stained with different antibody pairs for occludin and ZO-1 (*A*), N-cadherin and β-catenin (*B*), JAM-A and ZO-1 (*C*) to visualize their localization at the BTB. *Bar* in *a* = 80 μm, which applies to remaining graphs. A transient loss in occludin, ZO-1, and N-cadherin, but not β-catenin or JAM-A, was readily detected (see *A–C*, *panels e–h versus panels a–d* and *i–l*). *DAPI*, 4,6-diamidino-2-phenylindole.

steady-state protein levels of CD2AP, Ras, and TβRI remained relatively stable except for a decline in TAB1 level by day 4 when lysates of these samples were analyzed (*right versus middle panel* in Fig. 7*E*, see also Fig. 7*F*). Fig. 7, *C* and *E, last panel in the left column,* shows the IgG heavy chain in the Co-IP experiment, illustrating equal protein loading and uniform protein transfer. In short, these data illustrate (see Fig. 8) that when CD2AP was associated with the TGF-β3-TβRI complex, the ERK signaling pathway was activated, leading to a *reversible* disruption of Sertoli germ cell adhesion without compromising the BTB. However, when TAB1 and CD2AP were both asso- F8

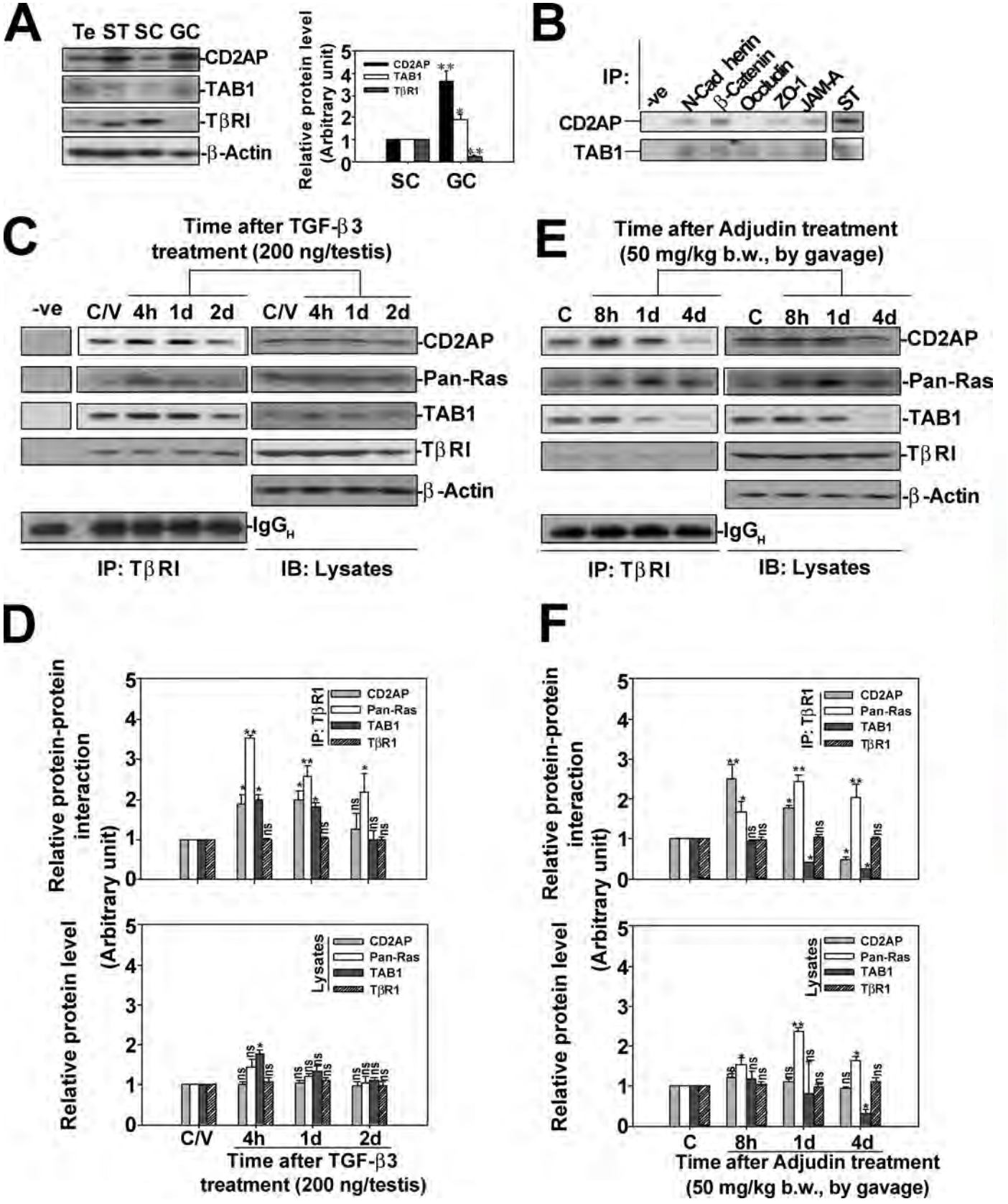

FIGURE 7. **TGF-β3 activates specific MAP kinases by recruiting different switching adaptors to the activated TβR1 in the testis.** *A,* immunoblots using lysates of testes (*Te*), seminiferous tubule (*ST*), Sertoli cells (*SC*), and germ cells (*GC*) showing relative abundance of two adaptors: CD2AP (80 kDa) and TAB1 (56 kDa) *versus* TβR1 (53 kDa) (*right panel*). β-Actin served as the protein loading control. The *left panel* is the histogram with $n = 4$ using different samples. *B,* interactions of typical BTB-associated proteins: N-cadherin, β-catenin, occludin, ZO-1, and JAM-A with CD2AP or TAB1 by Co-IP using seminiferous tubule lysates. *C,* protein lysates (~500 μg of protein/sample) from TGF-β3-treated testes were used for Co-IP with an anti-TβR1 antibody during BTB restructuring, and the blot was probed for CD2AP, Ras (21 kDa), TAB1, and TβR1. Protein lysates (100 μg of protein/lane) without Co-IP (see *right panel*) or with normal rabbit IgG served as positive and negative controls, and β-actin and IgG$_H$ served as protein loading controls which also illustrated uniform

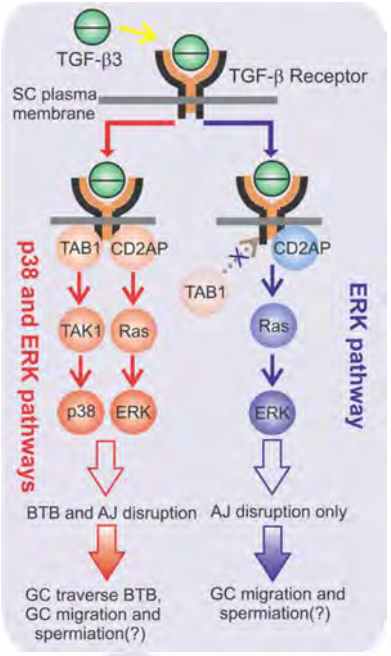

FIGURE 8. **A schematic drawing that illustrates the intriguing association between CD2AP, TAB1, and TβR1 (type 1 receptor for TGF-β) can selectively disrupt BTB and Sertoli germ cell adhesion or Sertoli germ cell adhesion alone.** This schematic drawing summarizes the results of the experiments reported herein. It illustrates that the differential interactions of TAB1 and CD2AP with the TGF-β3-TβR1 complex in the seminiferous epithelium can activate downstream signal transducers p38 and/or ERK. For instance, the association of the TGF-β3-TβR1 complex with adaptors TAB1 and CD2AP activates both p38 and/or ERK, perturbing BTB and AJ. However, if this protein complex only associates with CD2AP but not TAB1, it activates only ERK, selectively perturbing AJ without compromising the BTB.

ciated with the TGF-β3-TβRI complex, both the p38 and the ERK signaling pathways were activated, which, in turn, led to a *transient* and *reversible* disruption of the BTB and Sertoli germ cell adhesion.

DISCUSSION

TGF-β3 Is a Crucial Regulator of Junction Dynamics Pertinent to Spermatogenesis—TGF-β3 regulates multiple testicular functions, such as Leydig and germ cell proliferation, extracellular matrix synthesis, testis development, and follicle-stimulating hormone action (for reviews see Refs. 13, 14, and 31–33). Recent studies have shown that TGF-β3 is predominantly expressed by Sertoli and germ cells at the BTB site in the seminiferous epithelium at stages, including VII–VIII, of the epithelial cycle (24) (see also Fig. 2), coinciding with the events of spermiation and the migration of preleptotene/leptotene spermatocytes across the BTB (4, 34). Subsequent studies using specific inhibitors against different MAP kinases have shown that TGF-β3 also regulates Sertoli cell TJ dynamics *in vitro* and *in vivo* via the p38 MAPK signaling pathway in studies involving cadmium (12, 24, 35), an environmental toxicant known to disrupt BTB (36, 37). These earlier findings coupled with the data reported herein have prompted us to speculate that at late stage VII through stage VIII of the epithelial cycle, Sertoli, and germ cells contribute to an elevated level of TGF-β3 by secreting this cytokine to the microenvironment at the BTB. In turn, this activates the TβRI residing on Sertoli cells, recruiting adaptors CD2AP and TAB1 to the BTB and further activating the p38 MAPK and ERK signaling pathways. The net result of this interaction reduces the protein levels of both occludin/ZO-1 and cadherins at the BTB, as well as cadherins at the apical ES, perturbing both the TJ barrier and Sertoli germ cell adhesion and thereby transiently disrupts BTB and apical ES to facilitate both preleptotene/leptotene spermatocyte migration across the BTB and spermiation at apical ES (see Fig. 8). Whereas at other stages of the epithelial cycle, CD2AP, but not TAB1, is predominantly recruited to the TGF-β3-TβR1 protein complex, and the ERK pathway is preferentially activated to perturb Sertoli germ cell adhesion to facilitate germ cell movement across the seminiferous epithelium without compromising the BTB integrity. In short, CD2AP and TAB1 work as molecular switches that turn "on" and "off" of the TGF-β3-mediated p38/ERK or ERK signaling pathways in coordination with the epithelial cycle during spermatogenesis. Needless to say, the detailed biochemical event that activates the downstream signaling pathways following the recruitment of the two adaptors to the microenvironment at BTB remains to be elucidated. It is obvious that other kinases and phosphatases are involved because adaptors are known to serve as platforms for signal transduction by recruiting other regulatory proteins to the site besides tethering the integral membrane proteins to the actin or intermediate-based cytoskeleton (38). Even though the BTB at the basal compartment and the apical ES at the luminal edge of the seminiferous epithelium are morphologically distinct entities, they are the integral ultrastructures at the opposite ends of adjacent Sertoli cells. This molecular "switching" mechanism thus provides the efficient means to regulate the differential cell junction restructuring event at the Sertoli and the Sertoli germ cell interface. This is also physiologically necessary, perhaps essential, because at least 30–50 germ cells at different stages of their development are intimately associated with a single Sertoli cell in the seminiferous epithelium (39). As such, extensive but rapid restructuring can take place along the entire Sertoli cell surface from the basal to the apical (*i.e.* adluminal) portions of the cell via this switching mechanism to open or close TJ and/or AJ. Furthermore, results reported herein have unraveled a new *in vivo* model to study BTB dynamics because the use of TGF-β3 administered locally to the testis for studying BTB dynamics has fulfilled several important criteria. First, TGF-β3 is a natural substance released by Sertoli and germ cells, unlike other models that sought the use of a toxicant, such as cadmium or glycerol. Second, its disruptive effects to the BTB integrity and germ cell loss is reversible, unlike the cadmium and glycerol models whose damaging effects to the BTB are irreversible (20, 37). The fact that both germ cells could repopulate the epithelium and the TGF-β3-induced BTB damage could be resealed suggest that the dose (*i.e.* 200 ng of TGF-β3 per testis) that was used was not cytotoxic, consistent with results of earlier *in vitro* studies (11, 24). In this context, one may argue that the amount of TGF-β3 that was administered to each test animal at 200 ng/testis might not have reflected the physiological level of TGF-β3 at the BTB at stage VII–VIII when preleptotene and leptotene spermatocyte migrate across the BTB. To address this possibility, at least in part, we had performed immunoblot analysis as described under "Experimental Procedures" to assess the relative level of TGF-β3 in adult rat testes. It was shown that each adult rat testis contained ~1.1 ± 0.2 μg of TGF-β3, illustrating the administered dose at 200 ng per testis is within the physiological range. Furthermore, target genes that are important to junction disruption as well as "resealing" can now be identified and studied by using this model. Third, the entire experiment took a relatively short period of time to complete, only ~28 days, which include TGF-β3 recombinant protein adminis-

AQ: G

protein transfers from blots onto nitrocellulose membranes. *D,* data shown in *C* were scanned and summarized in these two histograms with $n = 3$. *E,* testis lysates (~500 μg of protein/sample) from adjudin-treated rats were used for Co-IP with an anti-TβRI antibody, and protein-protein interactions between TβR1 and CD2AP, Ras, or TAB1 were examined by immunoblottings (*left panel*). Protein lysates without Co-IP was shown in the *right panel. F,* histograms using data shown in *E* with $n = 3$. *ns*, not significantly different by ANOVA; *, $p < 0.05$; **, $p < 0.01$; *h,* hour; *d*, day.

tration, transient BTB and Sertoli germ cell adhesion damage, and full recovery (*e.g.* germ cell repopulation) in the testis. Thus, the experimental protocol is not time consuming, and it does not require the use of sophisticated equipment.

Adaptors TAB1 and CD2AP Are Molecular Switches in the Testis That Select the Downstream Signal Transducer of TGF-β3 to Reversibly Disrupt BTB and AJ via p38 MAPK or AJ Alone via ERK—In this context, it is of interest to note that TAB1 is an adaptor that is known to be expressed in almost all tissues examined to date, including the testis, and it is known to interact with TAK1 (TGF-β-activated kinase 1) to facilitate the activation of TAK1 by TGF-β receptors (40). CD2AP was originally identified as an adaptor that facilitated the formation of specialized junctions between T cells and antigen-presenting cells (41) and was found to be essential to maintain renal glomerulus epithelial junctions, known as the slit diaphragm, because CD2AP$^{-/-}$ mice died from renal failure by ~6 weeks postpartum (42). Interestingly, restoring the expression of CD2AP in the kidney was shown to prolong the life expectancy of these knock-out mice, yet the aging testes displayed progressive defects in spermatogenesis, possibly as a result of BTB breakdown (30). In the kidney, CD2AP preferentially directs TGF-β-mediated signaling to ERK instead of p38 MAPK (43), and this mechanism was shown to be used by the testis to transmit TGF-β3-induced signaling to regulate Sertoli germ cell adhesion as reported herein without perturbing the BTB (see Fig. 8) (14). It is likely that the lack of CD2AP in the seminiferous epithelium in these CD2AP knock-out mice can plausibly skew the TGF-β3-mediated signals toward the p38 MAPK pathway, and this thus disrupts the BTB, leading to defects in spermatogenesis as earlier reported (30). CD2AP has been shown to interact with multiple regulatory partners, such as phosphatidylinositol 3-kinase, p130 Cas, and proteins related to actin dynamics and endocytosis (44), and these kinases (*e.g.* phosphatidylinositol 3-kinase and c-Src) have been shown to be putative regulators of Sertoli germ cell adhesion in the rat testis (16). The demonstration that CD2AP interacts with N-cadherin, β-catenin, and ZO-1, but not occludin, at the BTB and with members in the TGF-β3/TβR1/ERK signaling cascade further strengthens the notion regarding the crucial role of CD2AP in junction dynamics in the testis. In this context, it is of interest to note that one can argue with the conclusion of this study because these results were acquired based on two relatively new models, namely the TGF-β3 model and the adjudin model in the field. However, studies that were based on these models have been validated using specific inhibitors against different signal transducers, such as SB202190 (a specific inhibitor of p38 MAPK (12, 35, 45)) and Y-27632 (a specific inhibitor ROCK inhibitor (46, 47, 48)) in the TGF-β3 and adjudin model, respectively. Needless to say, future studies should include an examination of TGF-β3-specific knock-out mice *versus* testis-specific overexpression of TGF-β3 regarding the status of BTB and spermatogenesis. Also, the levels of TGF-β3 in staged tubules at VII–VIII should also be quantified *versus* other stages. Nonetheless, results presented herein have shown that these models can now be used by investigators in the field to study junction dynamics pertinent to germ cell movement across the BTB, as well as from the basal compartment to the luminal edge of the seminiferous tubule during spermatogenesis.

Summary and Conclusions—As reported herein, the TGF-β3-TβR1-TAB1-CD2AP protein complex is one of the crucial regulatory protein complexes that induces transient disruption of BTB to facilitate preleptotene and leptotene spermatocyte migration across the BTB and the release of fully developed spermatids at spermiation by perturbing apical ES (see Fig. 8). It is obvious that this work should be expanded in future studies to prepare transgenic mice in which Sertoli cell TGF-β3 can be switched on and off to examine the subsequent effects on BTB function. Furthermore, results reported in this paper have shown that *in vivo* administration of TGF-β3 to adult rat testes is a novel model for studying BTB dynamics. In this context, it is of interest to note that other members of the TGF-β family, and perhaps other cytokines, may work in concert with TGF-β3 to regulate BTB dynamics during spermatogenesis (for a review see Ref. 14). For instance, earlier *in vitro* studies have shown that the assembly of Sertoli cell TJ permeability barrier *in vitro* was also associated with a decline in the steady-state TGF-β2 mRNA level (11). Additionally, Sertoli and germ cells are known to produce an array of cytokines both *in vitro* and *in vivo* (25, 49). This possibility should be carefully evaluated in future studies.

REFERENCES

1. Mruk, D. D., and Cheng, C. Y. (2004) *Trends Endocr. Metab.* **15,** 439–447
2. Wong, C. H., and Cheng, C. Y. (2005) *Curr. Top Dev. Biol.* **71,** 263–296
3. Mruk, D. D., and Cheng, C. Y. (2004) *Endocr. Rev.* **25,** 747–806
4. Russell, L. D. (1977) *Am. J. Anat.* **148,** 313–328
5. Pelletier, R. M., and Byers, S. W. (1992) *Microsc. Res. Tech.* **20,** 3–33
6. Dym, M., and Fawcett, D. W. (1970) *Biol. Reprod.* **3,** 308–326
7. Chung, N., and Cheng, C. Y. (2001) *Endocrinology* **142,** 1878–1888
8. Janecki, A., Jakubowiak, A., and Steinberger, A. (1992) *Toxicol. Appl. Pharmacol.* **112,** 51–57
9. Xia, W., Wong, C. H., Lee, N. P. Y., Lee, W. M., and Cheng, C. Y. (2005) *J. Cell. Physiol.* **205,** 141–157
10. Yan, H. H. N., and Cheng, C. Y. (2005) *Proc. Natl. Acad. Sci. U. S. A.* **102,** 11722–11727
11. Lui, W. Y., Lee, W. M., and Cheng, C. Y. (2001) *Endocrinology* **142,** 1865–1877
12. Wong, C. H., Mruk, D. D., Lui, W. Y., and Cheng, C. Y. (2004) *J. Cell Sci.* **117,** 783–798
13. Skinner, M. K. (1993) in *The Sertoli Cell* (Russell, L. D., and Griswold, M. D., eds) Cache River, Clearwater, FL
14. Xia, W., Mruk, D. D., Lee, W. M., and Cheng, C. Y. (2005) *Cytokine Growth Factor Rev.* **16,** 469–493
15. Xia, W., and Cheng, C. Y. (2005) *Dev. Biol.* **280,** 321–343
16. Siu, M. K. Y., Wong, C. H., Lee, W. M., and Cheng, C. Y. (2005) *J. Biol. Chem.* **280,** 25029–25047
17. Xu, H., Miller, J., and Bruce, T. L. (1992) *Nucleic Acids Res.* **20,** 6425–6426
18. Kiefer, K., Clement, J., Garidel, P., and Peschka-Suss, R. (2004) *Pharmacol. Res.* **21,** 1009–1017
19. Russell, L. D., Saxena, N. K., and Weber, J. E. (1987) *Gamete Res.* **17,** 43–56
20. Wiebe, J., Kowalik, A., Gallardi, R., Egeler, O., and Clubb, B. (2000) *J. Androl.* **21,** 625–635
21. Cheng, C. Y., Mruk, D., Silvestrini, B., Bonanomi, M., Wong, C. H., Siu, M. K. Y., Lee, N. P. Y., Lui, W. Y., and Mo, M. Y. (2005) *Contraception* **72,** 251–261
22. Lee, N. P. Y., Mruk, D. D., Conway, A. M., and Cheng, C. Y. (2004) *J. Androl.* **25,** 200–215
23. Bradford, M. (1976) *Anal. Biochem.* **72,** 248–254
24. Lui, W. Y., Lee, W. M., and Cheng, C. Y. (2003) *Biol. Reprod.* **68,** 1597–1612
25. Skinner, M. (1993) in *The Sertoli Cell* (Russell, L. D., and Griswold, M. D., eds) pp. 238–247, Cache River, Clearwater, FL
26. Ozaki-Kuroda, K., Nakanishi, H., Ohta, H., Tanaka, H., Kurihara, H., Mueller, S., Irie, K., Ikeda, W., Sakai, T., Wimmer, E., Nishimune, Y., and Takai, Y. (2002) *Curr. Biol.* **12,** 1145–1150
27. Chung, N. P. Y., Mruk, D., Mo, M.-Y., Lee, W. M., and Cheng, C. Y. (2001) *Biol. Reprod.* **65,** 1340–1351
28. Shi, Y., and Massague, J. (2003) *Cell* **113,** 685–700
29. Massague, J. (2000) *Nat. Rev. Mol. Cell Biol.* **1,** 169–178
30. Grunkemeyer, J. A., Kwoh, C., Huber, T. B., and Shaw, A. S. (2005) *J. Biol. Chem.* **280,** 29677–29681
31. Chang, H., Brown, C. W., and Matzuk, M. M. (2002) *Endocr. Rev.* **23,** 787–823
32. Gnessi, L., Fabbri, A., and Spera, G. (1997) *Endocr. Rev.* **18,** 541–609
33. Lui, W. Y., Lee, W. M., and Cheng, C. Y. (2003) *Int. J. Androl.* **26,** 1–14
34. Vogl, A. W., Pfeiffer, D. C., Mulholland, D., Kimel, G., and Guttman, J. (2000) *Arch. Histol. Cytol.* **63,** 1–15
35. Lui, W. Y., Wong, C. H., Mruk, D. D., and Cheng, C. Y. (2003) *Endocrinology* **144,** 1139–1142
36. Setchell, B. P., and Waites, G. M. H. (1970) *J. Endocrinol.* **47,** 81–86
37. Hew, K. W., Heath, G. L., Jiwa, A. H., and Welsh, M. J. (1993) *Biol. Reprod.* **49,** 840–849
38. Pawson, T., and Nash, P. (2003) *Science* **300,** 445–452
39. Weber, J. E., Russell, L. D., Wong, V., and Peterson, R. N. (1983) *Am. J. Anat.* **167,**

AQ: H

AQ: I

163–179
40. Shibuya, H., Yamaguchi, K., Shirakabe, K., Tonegawa, A., Gotoh, Y., Ueno, N., Irie, K., Nishida, E., and Matsumoto, K. (1996) *Science* **272,** 1179–1182
41. Dustin, M. L., Olszowy, M. W., Holdorf, A. D., Li, J., Bromley, S., Desai, N., Widder, P., Rosenberger, F., van der Merwe, P. A., Allen, P. M., and Shaw, A. S. (1998) *Cell* **94,** 667–677
42. Shih, N.-Y., Li, J., Karpitskii, V., Nguyen, A., Dustin, M. L., Kanagawa, O., Miner, J. H., and Shaw, A. S. (1999) *Science* **286,** 312–315
43. Schiffer, M., Mundel, P., Shaw, A. S., and Bottinger, E. P. (2004) *J. Biol. Chem.* **279,** 37004–37012
44. Welsch, T., Endlich, N., Gokce, G., Doroshenko, E., Simpson, J. C., Kriz, W., Shaw, A. S., and Endlich, K. (2005) *Am. J. Physiol.* **289,** F1134–F1143
45. Ravanti, L., Hakkinen, L., Larjava, H., Saarialho-Kere, U., Foschi, M., Han, J., and Kahari, V. (1999) *J. Biol. Chem.* **274,** 37292–37300
46. Uehata, M., Ishizaki, T., Satoh, H., Ono, T., Kawahara, T., Morishita, T., Tamkawa, H., Yamagami, K., Inui, J., Maekawa, M., and Narumiya, S. (1997) *Nature* **389,** 990–994
47. Murata, T., Arii, S., Nakamura, T., Mori, A., Kaido, T., Furuyama, H., Furumoto, K., Nakao, T., Isobe, N., and Imamura, M. (2001) *J. Hepatol.* **35,** 474–481
48. Lui, W. Y., Lee, W. L., and Cheng, C. Y. (2003) *Biol. Reprod.* **68,** 2189–2206
49. Mruk, D. D., and Cheng, C. Y. (2000) in *Testis, Epididymis, and Technologies in the Year 2000* (Jegou, B., Pineau, C., and Saez, J., eds) pp. 197–228, Springer-Verlag, Berlin
50. Gronning, L. M., Knutsen, H. K., Eskild, W., Hansson, V., Tasken, K., and Tasken, K. A. (1999) *Eur. J. Endocrinol.* **141,** 75–82
51. Chaudhary, J., Johnson, J., Kim, G., and Skinner, M. K. (2001) *Endocrinology* **142,** 1727–1736
52. Anway, M. D., Johnston, D. S., Crawford, D., and Griswold, M. D. (2001) *Biol. Reprod.* **65,** 1289–1296
53. Hong, C. Y., Park, J. H., Seo, K. H., Kim, J.-M., Im, S. Y., Lee, J. W., Choi, H. S., and Lee, K. (2003) *Mol. Cell. Biol.* **23,** 6000–6012

AUTHOR QUERIES

AUTHOR PLEASE ANSWER ALL QUERIES 1

A—Au: To ensure proper indexing of names, confirm the following are the last names: Xia, Lee, and Cheng. If these are not the last names, please indicate last names here. Provide postal code for the Hong Kong affiliation.

B—Au/ Journal guidelines state that the summary should fit into the left-hand column. If summary is long enough to run over into the right-hand column, please cut text.

C—Au: Restriction enzymes are now in roman type per Nomenclature Committee, Nucleic Acids Research, 2003, Vol. 31, pp. 1805-1812.

D—Au: Journal does not abbreviate days.

E—Au the citation to Supplemental Table 1 was deleted because there is no supplemental material in the accepted version of "Papers in Press."

F—Au no arrows in Fig. 4F, confirm change to "*black arrowheads* in Fig. 4*F*".

G—Au: quotes are deleted after the first usage per journal style.

H—Au: In ref. 13, please provide page range. Please confirm publisher and location.

I—Au: In ref. 25, please confirm name of publisher and provide location of publisher.

J—Au: Please check all color figures and note clearly any concerns about color reproduction. Color figures supplied by the author as RGB remain RGB in your page proofs and in online publication but may experience a color shift in the printed version of the journal. For more information please see: http://art.cadmus.com/da/jbc/guidelines_rgb.jsp If color corrections are needed, please include the revised RGB file on a zip disk or CD when you return the page proofs.